P-ISSN 2586-9000
E-ISSN 2586-9027
Homepage : *https://tci-thaijo.org/index.php/SciTechAsia* Science & Technology Asia
Vol. 23 No.2 April - June 2018 Page: [66 – 85]
Original research article

Sampled-data Modeling of a Single-Ended Primary Inductor Converter in Discontinuous Conduction Mode

Yossawee Weerakamhaeng[1,*]
[1]*Faculty of Engineering, Department of Electrical and Computer Engineering, Thammasat University, Pathum Thani 12120, Thailand*

Received 26 February 2018; Received in revised form 19 May 2018
Accepted 30 May 2018; Available online 30 June 2018

ABSTRACT

This paper presents the small-signal modeling of a Single-Ended Primary Inductor Converter power stage operating in discontinuous conduction mode using the sampled-data modeling technique. In addition, two algebraic manipulating features are revealed; the simpler periodic solution determination by the concept of Volt-Second and Capacitor-Charge balance, and the replacement of the expression involving the singular matrix by the equivalent function with the $s-$domain matrix. Four pulse transfer functions are derived from the model: the small-signal input-to-output voltage pulse transfer function, the small-signal duty duration-to-output voltage pulse transfer function, the input-to-output voltage pulse transfer function, and the duty duration-to-output voltage pulse transfer function. The model verification is analyzed by the simulation results. The response sequences from the pulse transfer functions oscillate by the same phase and frequency to the one from the simulation with slightly peak amplitude differences, confirming the validity of the acquired pulse transfer functions.

Keywords: Sampled-data control system; SEPIC converter modeling; Discontinuous conduction mode converter; Discretization.

1. Introduction

The Single-Ended Primary Inductor Converter(SEPIC) operated in the discontinuous conduction mode(DCM) has been extensively adopted as a power factor preregulator(PFP) [1] in off-line power supplies that stay in a distributed power system. Most power supply usages range from battery charging, appliance power sources and so on. Traditional off-line power supplies use a diode full bridge rectifier and large value of input filter capacitor at the input part. With this configuration, when an off-line power supply is turned on, a line

***Corresponding author**: cgsiit@gmail.com **doi:** 10.14456/scitechasia.2018.16

current with huge amount of excessive peaks is drawn from the power system line. As a result, this produces a high level of total harmonic distortion(THD) on the line, leading to a deteriorated power factor. In order to improve the power factor close to unity and reduce the percentage of THD, several types of passive and active power factor correction(PFC) schemes have been proposed. Passive PFC schemes do not lend themselves to this application due to the expense for each bulky component in the circuit and all the components being suitable for only a particular frequency. Accordingly, an adaptive PFC technique known as Active Power Factor Correction(APFC) comes into play. In APFC, the duty ratio as the switching parameter of dc-dc converters is controlled so that the dc-dc converter behaves as if it were a resistive load of the distributed power system. By operating at a high switching frequency, the size of the reactive elements gets reduced. This advantage makes it suitable for PFC applications.

Controlling the duty ratio of the switching element of a SEPIC so that the input current is in-phase with the input line voltage requires the more consistent model of a SEPIC. Two major approaches in implementing control circuits in PFP are described in [1] as the multiplier approach and voltage-follower approach. Several modeling techniques were proposed to model a SEPIC. These are the state-space averaging technique, the circuit averaging technique, the discrete modeling technique and the sampled-data modeling technique. According to [2], the state-space averaging technique is based on analytical averaging of state-space equations describing linear equivalent circuits for different states of a converter determined by the on-off status of the switching elements, whereas, the circuit averaging method leads to linear circuit models but emphasizes the average values of voltages and currents rather than their instantaneous values. For the state-space averaging technique proposed by [3], a linearized model based on this method is suitable when switching converters operate in continuous conduction mode(CCM) with low frequency of interest, but exhibit large discrepancies between the model and the measured behavior in the decade immediately below the Nyquist frequency and is unable to predict the well-known sub-harmonic oscillation [4,5]. In order to be accurate at the high frequency, [6] proposed the discrete modeling technique. The linearized model obtained from this technique produces the accurate response sequence at both low and high frequency ranges but lacks the continuous nature of the converter waveform. To compensate between merits and demerits of the former techniques, the sampled-data modeling technique [4] was introduced. This method gives rise to the model that incorporates both the continuous form of the state-space averaged model and the high-frequency accuracy of the discrete model.

PFP by the voltage-follower approach is mentioned in [7] with the analysis in the steady-state condition. Several studies [8-11] do the analysis by modeling a SEPIC in DCM using the state-space averaging technique. Even though there are various dc-dc converters being modeled with the sampled-data modeling technique in continuous conduction mode(CCM), such as a switched-capacitor voltage regulator [12], a boost or buck converter [13,14], it is rare to discover the modeling and analysis of a SEPIC in DCM using the sampled-data modeling technique. As a result, this study demonstrates the modeling of a non-isolated SEPIC in DCM with adjustable output voltage using the sampled-data modeling technique. The model verification of the pulse transfer function is analyzed by comparing with the simulation results. The response sequences from the pulse transfer functions oscillate by the same phase and frequency to the one from the simulation with slightly peak amplitude differences, confirming the validity of the acquired pulse transfer functions.

2. Sampled-data Modeling of an Open Loop SEPIC in DCM

A typical non-isolated SEPIC circuit can be illustrated as in Fig. 1.

2.1 Switching State Description :

For a SEPIC, the switching component is controlled by a pulse-width modulator (PWM). The state of the switching component is completely determined by a switching function $d(t)$ which is defined as [4]

$$d(t)=\begin{cases}1 \ if \ \ t\in \ \ \left[nT_s,\left(n+d_n\right)T_s\right)\\ 0 \ if \ \ t\in \left[\left(n+d_n\right)T_s,\left(n+1\right)T_s\right)\end{cases} \tag{2.1}$$

Where the duty ratio d_n is the fractional quantity, $0\le d_n\le 1$. The n^{th} switching cycle is denoted as $\left[t_n,t_n+T_s\right]$ where T_s is the duration of the n^{th} switching cycle. Within one switching cycle, $d(t)$ of Equation (2.1) has two

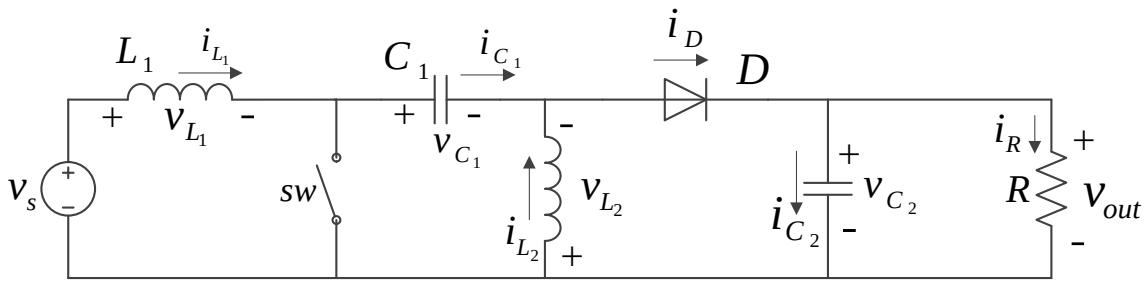

Fig. 1. A typical non-isolated SEPIC circuit.

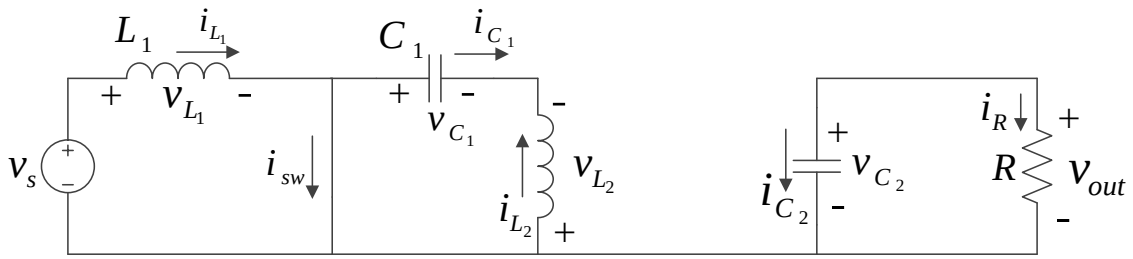

Fig. 2. An equivalent SEPIC circuit in S_1-state.

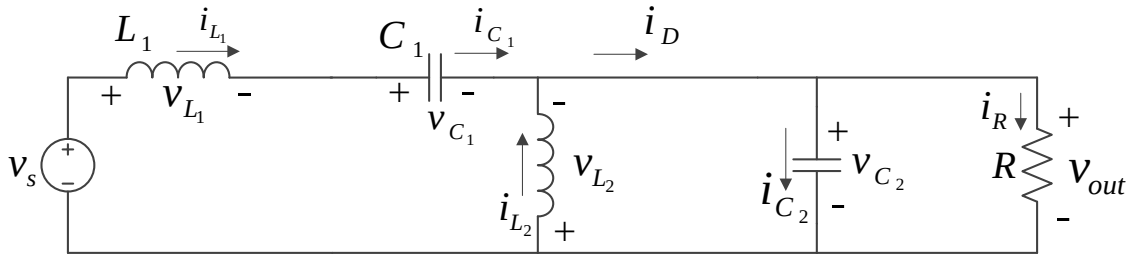

Fig. 3. An equivalent SEPIC circuit in S_2-state.

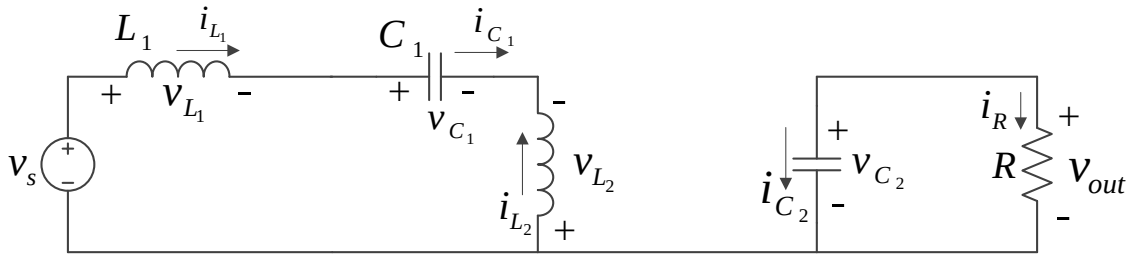

Fig. 4. An equivalent SEPIC circuit in S_3-state.

different values, whereas a SEPIC in DCM traverses consecutively into 3 different states, S_1-state, S_2- state and S_3-state as shown in Fig. 2, Fig. 3 and Fig. 4 respectively. In the S_i-state, the duty duration $\beta_{i,n}(d_{i,n})$ in that state is defined as :

$$\beta_{i,n}(d_{i,n}) = d_{i,n}T_s \quad for\ i = 1,2,3 \tag{2.2}$$

Where :

$$d_{i,n} = d_n \quad if \quad i = 1 \tag{2.3}$$

$$\sum_{i=1}^{3} d_{i,n} \quad = 1 \tag{2.4}$$

2.2 The Methodology of the Sampled-data Modeling Technique :

The general method of the sampled-data modeling technique has four main steps [12]

2.2.1 Expression of large-signal dynamics :

The SEPIC in DCM consists of three states; S_1, S_2 and S_3, each of which can be represented by the state space representation as follows.

2.2.1.1 S_1-state:

when $t \in \left[nT_s, \left(n + d_{1,n}\right)T_s \right)$,

a SEPIC comes into S_1 state where

$$S_1 : \begin{cases} \dot{x}(t) = A_1 x(t) + B_1 u(t) \\ v_{out}(t) = C_1 x(t) + D_1 u(t) \end{cases} \tag{2.5}$$

2.2.1.2 S_2-state:

when $t \in \left[\left(n + d_{1,n}\right)T_s, \left(n + d_{2,n}\right)T_s \right)$, a SEPIC comes into S_2 state where

$$S_2 : \begin{cases} \dot{x}(t) = A_2 x(t) + B_2 u(t) \\ v_{out}(t) = C_2 x(t) + D_2 u(t) \end{cases} \tag{2.6}$$

2.2.1.3 S_3-state:

when $t \in \left[\left(n + d_{2,n}\right)T_s, \left(n+1\right)T_s \right)$, a SEPIC comes into S_3 state where

$$S_3 : \begin{cases} \dot{x}(t) = A_3 x(t) + B_3 u(t) \\ v_{out}(t) = C_3 x(t) + D_3 u(t) \end{cases} \tag{2.7}$$

$u(t)$ is the input vector which is often the supply voltage v_s and $x(t) = \left[i_{L1}(t) \quad i_{L2}(t) \quad v_{C1}(t) \quad v_{C2}(t) \right]^T$ is the state variable vector of the system for the case of a SEPIC. The sampling period T_s is chosen as such a small period that $u(t) = u(nT_s)$ for $t \in \left[nT_s, \left(n+1\right)T_s \right)$. Let x_n and x_{n+1} be state vectors at time t_n and $t_n + T_s$ in consequence and u_n be the input vector at t_n. $A_1, A_2, A_3, B_1, B_2, B_3, C_1, C_2, C_3, D_1, D_2$ and D_3 are defined as follows.

$$A_1 = \begin{bmatrix} 0 & 0 & 0 & 0 \\ 0 & 0 & \frac{1}{L_2} & 0 \\ 0 & -\frac{1}{C_1} & 0 & 0 \\ 0 & 0 & 0 & -\frac{1}{C_2 R} \end{bmatrix} \tag{2.8}$$

$$A_2 = \begin{bmatrix} 0 & 0 & -\frac{1}{L_1} & -\frac{1}{L_1} \\ 0 & 0 & 0 & -\frac{1}{L_2} \\ \frac{1}{C_1} & 0 & 0 & 0 \\ \frac{1}{C_2} & \frac{1}{C_2} & 0 & -\frac{1}{C_2 R} \end{bmatrix} \tag{2.9}$$

$$A_3 = \begin{bmatrix} 0 & 0 & -\dfrac{1}{L_1+L_2} & 0 \\ 0 & 0 & \dfrac{1}{L_1+L_2} & 0 \\ \dfrac{1}{C_1} & 0 & 0 & 0 \\ 0 & 0 & 0 & -\dfrac{1}{C_2R} \end{bmatrix} \quad (2.10)$$

$$B_1 = \begin{bmatrix} \dfrac{1}{L_1} \\ 0 \\ 0 \\ 0 \end{bmatrix}, B_2 = \begin{bmatrix} \dfrac{1}{L_1} \\ 0 \\ 0 \\ 0 \end{bmatrix}, B_3 = \begin{bmatrix} \dfrac{1}{L_1+L_2} \\ -\dfrac{1}{L_1+L_2} \\ 0 \\ 0 \end{bmatrix} \quad (2.11)$$

$$C_1 = C_2 = C_3 = \begin{bmatrix} 0 & 0 & 0 & 1 \end{bmatrix}, \quad D_1 = D_2 = D_3 = \begin{bmatrix} 0 \end{bmatrix} \quad (2.12)$$

With the ensuing section, it can be seen that $\beta_{2,n} = \beta_{2,n}(\beta_{1,n})$ and $\beta_{3,n} = \beta_{3,n}(\beta_{1,n})$ are functions of $\beta_{1,n}$. In addition, at any t, the solution $x(t)$ of Equation (5), (6) and (7) as the state transition equations combining $x_n = x(nT_s)$ to $x_{n+1} = x((n+1)T_s)$ can be expressed as

$$\begin{aligned} x_{n+1} &= f\left(x_n, u_n, \beta_{1,n}\right) \\ &= \Phi\left(\beta_{1,n}\right) x_n + \Gamma\left(\beta_{1,n}\right) u_n \end{aligned} \quad (2.13)$$

Where :

$$\begin{aligned} \Phi_i\left(\beta_{i,n}\right) &= e^{A_i \beta_{i,n}} \\ &= L^{-1}\left\{ \left[sI - A_i \right]^{-1} \right\} \Big|_{t=\beta_{i,n}} \end{aligned} \quad (2.14)$$

$$\Phi\left(\beta_{1,n}\right) = \Phi_3\left(\beta_{3,n}\right)\Phi_2\left(\beta_{2,n}\right)\Phi_1\left(\beta_{1,n}\right) \quad (2.15)$$

$$\Gamma_i\left(\beta_{i,n}\right) = \begin{cases} \left(\int_0^{\beta_{i,n}} e^{A_i \alpha}\, d\alpha \right) B_i = \left[e^{A_i \beta_{i,n}} - I \right] A_i^{-1} B_i = A_i^{-1} \left[e^{A_i \beta_{i,n}} - I \right] B_i & \text{if } A_i \text{ is invertible} \\ \left[L^{-1}\left\{ \left[sI - A_i \right]^{-1} \left[\dfrac{1}{s} \right] \right\} \Big|_{t=\beta_{i,n}} \right] B_i & \text{if } A_i \text{ is singular} \end{cases} \quad (2.16)$$

$$\Gamma\left(\beta_{1,n}\right) = \Phi_3\left(\beta_{3,n}\right)\Phi_2\left(\beta_{2,n}\right)\Gamma_1\left(\beta_{1,n}\right) + \Phi_3\left(\beta_{3,n}\right)\Gamma_2\left(\beta_{2,n}\right) + \Gamma_3\left(\beta_{3,n}\right) \quad (2.17)$$

2.2.2 Evaluation of steady-state conditions and expression of the periodic converter behavior including condition for discontinuous conduction mode(DCM) of operation :

A steady-state operating condition is the condition when $x_{n+1} = x_n$. The system in this operating condition possesses the state vector x_n as a periodic solution [2]. For a system subject to the sampling period of T_s, a periodic solution is sometimes called a T_s – periodic solution corresponding to a fixed-point steady-state solution $\left(x_{ss}\left(u^{ss}, \beta_1^{ss}, T_s\right), \beta_1^{ss}, T_s\right)$ where $x_{ss}\left(u^{ss}, \beta_1^{ss}, T_s\right)$ is the fixed-point steady-state vector being a function of u^{ss}, β_1^{ss} and T_s.

u^{ss} is the fixed-point steady-state input vector, β_1^{ss} is the fixed-point steady-state duty duration in the S_1 state.

By setting $u^{ss} = v_s$, determining $x_{ss}\left(u^{ss}, \beta_1^{ss}, T_s\right)$ where $x^{ss} = \left[i_{L1}^{ss}(\beta_1^{ss}) \quad i_{L2}^{ss}(\beta_1^{ss}) \quad v_{C1}^{ss}(\beta_1^{ss}) \quad v_{C2}^{ss}(\beta_1^{ss})\right]^T$, β_1^{ss} , β_2^{ss} and β_3^{ss} can be achieved by the concept of Volt-Second and Capacitor-Charge balance from power electronics courses and the DCM condition [15] as follows

$$\Delta i_{L1}\big|_{S_1-state} + \Delta i_{L1}\big|_{S_2-state} + \Delta i_{L1}\big|_{S_3-state} \approx \left(\frac{di_{L1}}{dt}\bigg|_{S_1-state}\right)\beta_1^{ss} + \left(\frac{di_{L1}}{dt}\bigg|_{S_2-state}\right)\beta_2^{ss} + \left(\frac{di_{L1}}{dt}\bigg|_{S_3-state}\right)\beta_3^{ss} = 0 \quad (2.18)$$

$$\Delta i_{L2}\big|_{S_1-state} + \Delta i_{L2}\big|_{S_2-state} + \Delta i_{L2}\big|_{S_3-state} \approx \left(\frac{di_{L2}}{dt}\bigg|_{S_1-state}\right)\beta_1^{ss} + \left(\frac{di_{L2}}{dt}\bigg|_{S_2-state}\right)\beta_2^{ss} + \left(\frac{di_{L2}}{dt}\bigg|_{S_3-state}\right)\beta_3^{ss} = 0 \quad (2.19)$$

$$\Delta v_{C1}\big|_{S_1-state} + \Delta v_{C1}\big|_{S_2-state} + \Delta v_{C1}\big|_{S_3-state} \approx \left(\frac{dv_{C1}}{dt}\bigg|_{S_1-state}\right)\beta_1^{ss} + \left(\frac{dv_{C1}}{dt}\bigg|_{S_2-state}\right)\beta_2^{ss} + \left(\frac{dv_{C1}}{dt}\bigg|_{S_3-state}\right)\beta_3^{ss} = 0 \quad (2.20)$$

$$\Delta v_{C2}\big|_{S_1-state} + \Delta v_{C2}\big|_{S_2-state} + \Delta v_{C2}\big|_{S_3-state} \approx \left(\frac{dv_{C2}}{dt}\bigg|_{S_1-state}\right)\beta_1^{ss} + \left(\frac{dv_{C2}}{dt}\bigg|_{S_2-state}\right)\beta_2^{ss} + \left(\frac{dv_{C2}}{dt}\bigg|_{S_3-state}\right)\beta_3^{ss} = 0 \quad (2.21)$$

$$i_{L1\min}\big|_{S_2-state} + i_{L2\min}\big|_{S_2-state} = 0 \quad (2.22)$$

$$T_s - \beta_1^{ss} - \beta_2^{ss} - \beta_3^{ss} = 0 \quad (2.23)$$

$$v_{C2}^{ss} - v_{out}^{ref} = 0 \quad (2.24)$$

Solving Eq. (2.18), (2.19), (2.20), (2.21), (2.22), (2.23) and (2.24) simultaneously, we obtain

$$\beta_1^{ss} = \left(\sqrt{\frac{2L_1L_2T_s}{R\left(L_1+L_2\right)}} \right) \frac{v_{out}^{ref}}{v_s} \tag{2.25}$$

$$\beta_2^{ss} = \left(\frac{v_s}{v_{out}^{ref}} \right) \beta_1^{ss} \tag{2.26}$$

$$\beta_3^{ss} = T_s - \beta_1^{ss} - \beta_2^{ss} \tag{2.27}$$

$$i_{L1}^{ss} = \frac{\left(v_{out}^{ref}\right)^2}{Rv_s} \tag{2.28}$$

$$i_{L2}^{ss} = \left(\frac{T_s - \beta_1^{ss}}{\beta_1^{ss}} \right) \frac{\left(v_{out}^{ref}\right)^2}{Rv_s} \tag{2.29}$$

$$v_{C1}^{ss} = v_s \tag{2.30}$$

$$v_{C2}^{ss} = v_{out}^{ref} \tag{2.31}$$

From Eq. (2.25) and (2.26), by the given values of L_1, L_2 and R with the DCM constraint of Eq. (2.22), β_2^{ss} can be expressed as

$$\beta_2^{ss} = \sqrt{\frac{2L_1L_2T_s}{R\left(L_1+L_2\right)}} \tag{2.32}$$

A SEPIC traverses from the CCM to the DCM when $\beta_3^{ss} \in \left(0, T_s - \beta_1^{ss} - \beta_2^{ss}\right]$ or from Eq. (2.23) and (2.32), the minimum value of β_1^{ss} that lastly preserve the SEPIC in CCM(imminently being into DCM) can be expressed as

$$\beta_{1CCM\_MIN}^{ss} = T_s - \sqrt{\frac{2L_1L_2T_s}{R\left(L_1+L_2\right)}} \tag{2.33}$$

And the maximum achievable output voltage for a SEPIC in DCM $v_{out\max\_DCM}^{ss}$ or $v_{C2\max\_DCM}^{ss}$ can be determined as follows :

$$v_{C2\max\_DCM}^{ss} = \left(\frac{\beta_{1CCM\_MIN}^{ss}}{\beta_2^{ss}} \right) v_s \tag{2.34}$$

Therefore, for a given dc voltage source v_s, the desired reference output voltage $v_{out}^{ref} = v_{C2}^{ss} \le v_{C2\max\_DCM}^{ss}$ must satisfy Eq. (2.33) in order to preserve a SEPIC in DCM.

2.2.3 The steady-state model linearization :

In order to linearize x_{n+1} around a fixed-point steady-state $\left(x_{ss}\left(u^{ss}, \beta_1^{ss}, T_s\right), \beta_1^{ss}, T_s\right)$ and input dc voltage source v_s (considering $u_n = v_s$), x_n must be determined first by applying a steady-state operating condition of $x_{n+1} = x_n$ to Eq. (2.13),

$$x_n^p = \left[I - \Phi\left(\beta_1^{ss}\right) \right]^{-1} \Gamma\left(\beta_1^{ss}\right) v_s \tag{2.35}$$

and then x_{n+1} can be determined from x_n by the state transition equations. The small-signal dynamics can be obtained by linearizing the large-signal dynamics around the fixed-point steady-state $\left(x_{ss}\left(u^{ss}, \beta_1^{ss}, T_s\right), \beta_1^{ss}, T_s\right)$ and input dc voltage source v_s. Let $x_n, u_n, \beta_{1,n}$ and v_{out} be the perturbed state vector, input vector, duty duration in the S_1-state and output voltage, respectively $\tilde{x}_n, \tilde{u}_n, \tilde{\beta}_{1,n}$ and $\tilde{v}_{out}$ are the perturbations of state vector, input vector, duty duration and output voltage sequentially. They are expressed as

$$x_n = x^{ss} + \tilde{x}_n, \quad u_n = u^{ss} + \tilde{u}_n,$$
$$\beta_{1,n} = \beta_1^{ss} + \tilde{\beta}_{1,n}, \quad v_{out} = v_{out}^{ref} + \tilde{v}_{out} \tag{2.36}$$

The small-signal model of this system can be represented as

$$\tilde{x}_{n+1} \approx \left.\frac{df}{dx_n}\right|_{(x^{ss},\beta_1^{ss},T_s)} \tilde{x}_n + \left.\frac{df}{du_n}\right|_{(x^{ss},\beta_1^{ss},T_s)} \tilde{u}_n + \left.\frac{df}{d\beta_{1,n}}\right|_{(x^{ss},\beta_1^{ss},T_s)} \tilde{\beta}_{1,n} \tag{2.37}$$

$$\tilde{v}_{out} \approx C_1\tilde{x}_n + D_1\tilde{u}_n \tag{2.38}$$

Where

$$\left.\frac{df}{dx_n}\right|_{(x^{ss},\beta_1^{ss},T_s)} = \Phi_3\left(\beta_3^{ss}\right)\Phi_2\left(\beta_2^{ss}\right)\Phi_1\left(\beta_1^{ss}\right) = \Phi\left(\beta_1^{ss}\right) \tag{2.39}$$

$$\left.\frac{df}{du_n}\right|_{(x^{ss},\beta_1^{ss},T_s)} = \Gamma\left(\beta_1^{ss}\right) \tag{2.40}$$

$$x^p(0) = x_n^p = \left[I - \Phi\left(\beta_1^{ss}\right)\right]^{-1}\Gamma\left(\beta_1^{ss}\right)u(0) = \left[I - \Phi\left(\beta_1^{ss}\right)\right]^{-1}\Gamma\left(\beta_1^{ss}\right)v_s \tag{2.41}$$

$$\dot{x}^p\left((0)^-\right) \approx A_3x^p(0) + B_3u(0) \tag{2.42}$$

$$\dot{x}^p\left((0)^+\right) \approx A_1x^p(0) + B_1u(0) \tag{2.43}$$

$$\dot{x}^p\left(\left(\beta_1^{ss}\right)^-\right) \approx A_1x^p\left(\beta_1^{ss}\right) + B_1u\left(\beta_1^{ss}\right) = A_1x^p\left(\beta_1^{ss}\right) + B_1u(0) \tag{2.44}$$

$$\dot{x}^p\left(\left(\beta_1^{ss}\right)^+\right) \approx A_2x^p\left(\beta_1^{ss}\right) + B_2u\left(\beta_1^{ss}\right) = A_2x^p\left(\beta_1^{ss}\right) + B_2u(0) \tag{2.45}$$

$$\dot{x}^p\left(\left(\beta_1^{ss} + \beta_2^{ss}\right)^-\right) \approx A_2x^p\left(\beta_1^{ss} + \beta_2^{ss}\right) + B_2u\left(\beta_1^{ss} + \beta_2^{ss}\right) \approx A_2x^p\left(\beta_1^{ss} + \beta_2^{ss}\right) + B_2u(0) \tag{2.46}$$

$$\dot{x}^{p}\left(\left(\beta_1^{ss}+\beta_2^{ss}\right)^{+}\right)\approx A_3 x^{p}\left(\beta_1^{ss}+\beta_2^{ss}\right)+B_3 u\left(\beta_1^{ss}+\beta_2^{ss}\right)$$
$$\approx A_3 x^{p}\left(\beta_1^{ss}+\beta_2^{ss}\right)+B_3 u(0) \quad (2.47)$$

$$\left.\frac{df}{d\beta_{1,n}}\right|_{(x^{ss},\beta_1^{ss},T_s)}=\left(-1-\frac{v_s}{v_{out}^{ref}}\right)\Phi_3(\beta_3^{ss})\dot{x}^{p}\left(\left(\beta_1^{ss}+\beta_2^{ss}\right)^{+}\right)$$
$$+\left(\frac{v_s}{v_{out}^{ref}}\right)\Phi_3(\beta_3^{ss})\Phi_2(\beta_2^{ss})\dot{x}^{p}\left(\left(\beta_1^{ss}\right)^{+}\right)$$
$$+\Phi_3(\beta_3^{ss})\Phi_2(\beta_2^{ss})\Phi_1(\beta_1^{ss})\dot{x}^{p}\left((0)^{+}\right) \quad (2.48)$$

Small-signal dynamics :

The small-signal input-to-output pulse transfer function $T_{vu}(z)$ and the small-signal duty duration-to-output pulse transfer function $T_{v\beta_1}(z)$ can be derived by applying the z-transform to Eq. (2.37) and Eq. (2.38).

$$T_{vu}(z)=\frac{\tilde{V}_{out}(z)}{\tilde{U}(z)}$$
$$=C_1\left[zI-\Phi\left(\beta_1^{ss}\right)\right]^{-1}\Gamma\left(\beta_1^{ss}\right)+D_1 \quad (2.49)$$

$$T_{v\beta_1}(z)=\frac{\tilde{V}_{out}(z)}{\tilde{\beta}_1(z)}$$
$$=C_1\left[zI-\Phi\left(\beta_1^{ss}\right)\right]^{-1}\Gamma_{\beta_1}\left(\beta_1^{ss}\right) \quad (2.50)$$

Steady-state dynamics :

When $n\to\infty$, with the constraints of $\tilde{x}_{n+1}=0$ and $\tilde{v}_{out}=0$, the dynamic model of a SEPIC in DCM with the imposed constraints is called the steady-state dynamics and it can be proved that

$$V_{out}(z)=T_{vu}(z)U(z)+T_{v\beta_1}(z)\beta_1(z) \quad (2.51)$$

With the constraint of $\tilde{v}_{out}=0$ when $n\to\infty$ and by the final value theorem, defining a scaling factor K_{final} such that

$$K_{final}=v_{out}^{ref}\left[\lim_{z\to 1}\left(1-z^{-1}\right)V_{out}(z)\right]^{-1} \quad (2.52)$$

The input-to-output pulse transfer function $G_{vu}(z)$ and the duty duration-to-output pulse transfer function $G_{v\beta_1}(z)$ are defined as follows :

$$G_{vu}(z)=K_{final}\frac{V_{out}(z)}{U(z)} \quad (2.53)$$

$$G_{v\beta_1}(z)=K_{final}\frac{V_{out}(z)}{\beta_1(z)} \quad (2.54)$$

Where $V_{out}(z)$ is from Eq. (2.51).

2.3 SEPIC dynamic model verification :

The dynamic models of a SEPIC represented by Eq. (2.49) and Eq. (2.50) are verified by comparing the step response of Eq. (2.49) when the input sequence is a step sequence $v_s u[n]$ and the step response of Eq. (2.50) when the input sequence is a step sequence $\beta_1^{ss}u[n]$, respectively, with the output response $v_{out}(nT_s)$ of the simulation(from the simulation diagram, consisting of components from MATLAB

simulink toolbox) of the relevant SEPIC model represented by Eq. (2.5), (2.6) and (2.7).

2.4 Eigenvalue stability analysis :

According to [3], the stability considered in this study is the relative stability of the linearized model of a SEPIC represented by Eq. (2.37) and (2.38). In a discrete time control system, a linear shift-invariant system is asymptotically stable when all of the poles or roots of the determinant $\left| zI - \Phi\left(\beta_1^{ss}\right)\right|$ or equivalently the eigenvalues of $\Phi\left(\beta_1^{ss}\right)$ are inside the unit circle in the complex z-plane. The locations of the eigenvalues in the z-plane convey the transient response of the system, i.e., damping and oscillation of the response.

3. Simulation results

A SEPIC with the following parameters is considered in this study.

$v_s = 8.0\ volt$, , $v_{out}^{ref} = 5.0\ volt$

, $L_1 = 100\ mH$, $L_2 = 100\ mH$

, $C_1 = 330.0\ \mu F$ $C_2 = 2200.0\ \mu F$

$R = 1\ k\Omega$ $f_s = \dfrac{1}{T_s} = 31.25\ kHz$

$T_s = 3.2\times10^{-5}\ s$. From Eq. (2.32), $\beta_2^{ss} = 1.7889\times10^{-5}\ s$, from Eq. (2.33), $\beta_{1CCM\_MIN}^{ss} = 1.4111\times10^{-5}\ s$ and the maximum achievable output voltage for a SEPIC in DCM $v_{out\max\_DCM}^{ss}$ or $v_{C2\max\_DCM}^{ss}$ can be determined from Equation (2.34) and $v_{C2\max\_DCM}^{ss} = 6.3108$ v. Therefore, it is possible for the desired reference output voltage $v_{out}^{ref} = 5.0\ v$ to operate the SEPIC in DCM. For a SEPIC in DCM, the steady-sate values $\beta_1^{ss}, \beta_2^{ss}, \beta_3^{ss}, i_{L1}^{ss}, i_{L1}^{ss}, v_{C1}^{ss}, v_{C2}^{ss}$ can be determined from Eq. (2.25) to Eq. (2.31).

$\beta_1^{ss} = 1.1180\times10^{-5}\ s$,

$\beta_2^{ss} = 1.7889\times10^{-5}\ s$,

$\beta_3^{ss} = 2.9311\times10^{-6}\ s$, $i_{L1}^{ss} = 0.0031\ A$,

$i_{L2}^{ss} = 0.0058\ A$, $v_{C1}^{ss} = 8.0\ v$,

$v_{C2}^{ss} = 5.0\ v$. $U(z) = \dfrac{v_s z}{z-1}$,

$\beta_1(z) = \dfrac{\beta_1^{ss} z}{z-1}$.

Small-signal dynamics :

The small-signal input-to-output pulse transfer function $T_{vu}(z)$ and the small-signal duty duration-to-output pulse transfer function $T_{v\beta_1}(z)$ can be calculated as

$$T_{vu}(z) = \frac{1.636\times10^{-5}\left(z^3 - 1.5556z^2 + 0.1112z + 0.4446\right)}{z^4 - 3.9998z^3 + 5.9996z^2 - 3.9998z + 1.0}$$

$$T_{v\beta_1}(z) = \frac{13.35\left(z^3 - 2.9985z^2 + 2.9985z - 0.9993\right)}{z^4 - 3.9998z^3 + 5.9996z^2 - 3.9998z + 1.0}$$

Steady-state dynamics :

From Eq. (2.52), $K_{final} = 1.0838$. The input-to-output pulse transfer function $G_{vu}(z)$ and the duty duration-to-output pulse transfer function $G_{v\beta_1}(z)$ are obtained as follows :

$$G_{vu}(z) = \frac{3.795\times10^{-5}\left(z^3 - 2.3246z^2 + 1.6498z - 0.3249\right)}{z^4 - 3.9998z^3 + 5.9996z^2 - 3.9998z + 1.0}$$

$$G_{v\beta_1}(z) = \frac{27.15\left(z^3 - 2.3252z^2 + 1.6501z - 0.3250\right)}{z^4 - 3.9998z^3 + 5.9996z^2 - 3.9998z + 1.0}$$

SEPIC dynamic model verification

$G_{vu}(z)$ was verified by comparing the step response sequence $v_{out}[n]$, when the input sequence $v_s\,u[n]$ applied, with the response $v_{out}\left(nT_s\right)$ from the simulation, whereas $G_{v\beta_1}(z)$ was verified by comparing the step response sequence $v_{out}[n]$, when the input sequence $\beta_1^{ss}\,u[n]$ applied, with the response $v_{out}\left(nT_s\right)$ from the simulation as in Fig. 6, Fig. 7 and Fig. 8. It can be noticed that the step response sequences $v_{out}[n]$ (red line) from $G_{vu}(z)$ and $G_{v\beta_1}(z)$ are the same for the input sequences $v_s\,u[n]$ and $\beta_1^{ss}\,u[n]$, respectively. $v_{out}(t)$ and $v_{out}\left(nT_s\right)$ from the simulation are the gray line. The observation reveals that $v_{out}[n]$ oscillates by the same phase and frequency as $v_{out}(t)$ from the simulation with slight peak amplitude differences that might be due to the decimal precision from the limited number of digits used in the calculations, confirming the validity of the small-signal dynamic models of a SEPIC converter represented by $T_{vu}(z)$ and $T_{v\beta_1}(z)$ respectively. $i_{L1}(t), i_{L2}(t), v_{C1}(t)$ and $v_{C2}(t)$ can be visualized from Fig. 3 to Fig. 6 accordingly.

Eigenvalue stability analysis :

Poles of $T_{vu}(z)$, $T_{v\beta_1}(z)$, $G_{vu}(z)$ and $G_{v\beta_1}(z)$ are at $0.9999151 \pm 0.012923i$, $0.99998 \pm 0.00519844i$ which are all inside the unit circle in the z-plane as can be seen in Fig. 9. Zeros of $T_{vu}(z)$ are at -0.444449, $0.999939 \pm 0.01049345i$. By the way, those pairs of complex conjugate poles are located very close to the rim of the unit circle. As a result, the output response $v_{out}[n]$ for the step input $\beta_{1,n} = \beta_1^{ss}u[n]$ is sinusoidally decayed to a steady-state value with the rate of decay determined by the longest radial distances of complex conjugate poles from the origin. This system is still relatively stable and behaves as an underdamped system.

4. Discussion and conclusion

This paper presents the small-signal modeling of a SEPIC power stage operating in DCM using the sampled-data modeling technique, compensating for the pros and cons of the state-space averaging and the discrete modeling techniques. This study proposes to determine the periodic solution at the steady-state condition by the concept of Volt-Second and Capacitor-Charge balance from power electronics courses that are much easier. Four pulse transfer functions are derived from the model: the small-signal input-to-output voltage pulse transfer function, the small-signal duty duration-to-output voltage pulse transfer function, the input-to-output voltage pulse transfer function, and the duty duration-to-output voltage pulse transfer function. The relative stability analysis is carried out by considering the pole locations or the locations of the eigenvalues relative to the unit circle in the $z-$plane. Moreover, those poles characterize the response of the system, i.e., damping and oscillation of the response. The steady-state dynamic models are also derived in order that the output responses can be used to verify the model by comparing with the simulation response. The response sequences from the pulse transfer functions oscillate by the same phase and frequency as the one from the simulation with slight peak amplitude

differences that might be due to the decimal precision from the limited number of digits used in the calculations, confirming the validity of the acquired pulse transfer functions. The maximum achievable output voltage for a SEPIC in DCM is also mentioned in this study. The small-signal dynamic models from this study are versatile for the upcoming sampled-data control system or discrete-time control system design and implementation.

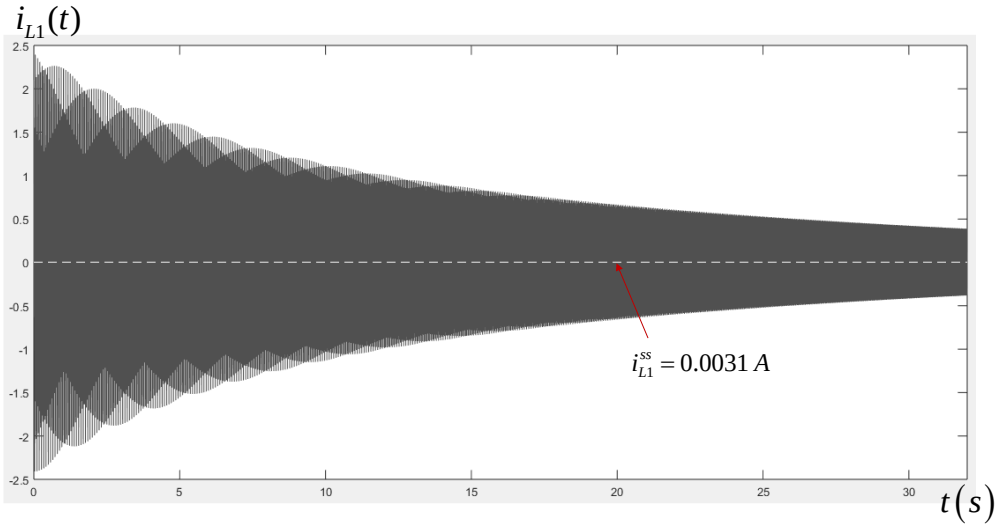

Fig. 5. $i_{L1}(t)$ of a SEPIC in DCM when $v_{out}^{ref} = 5.0\ v$ and $v_s = 8.0\ v$

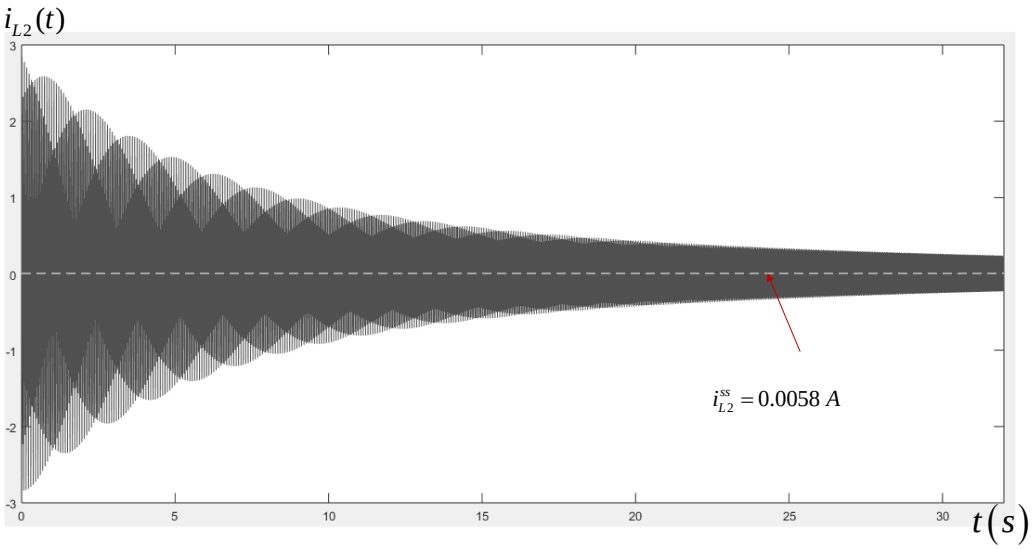

Fig. 6. $i_{L2}(t)$ of a SEPIC in DCM when $v_{out}^{ref} = 5.0\ v$ and $v_s = 8.0\ v$

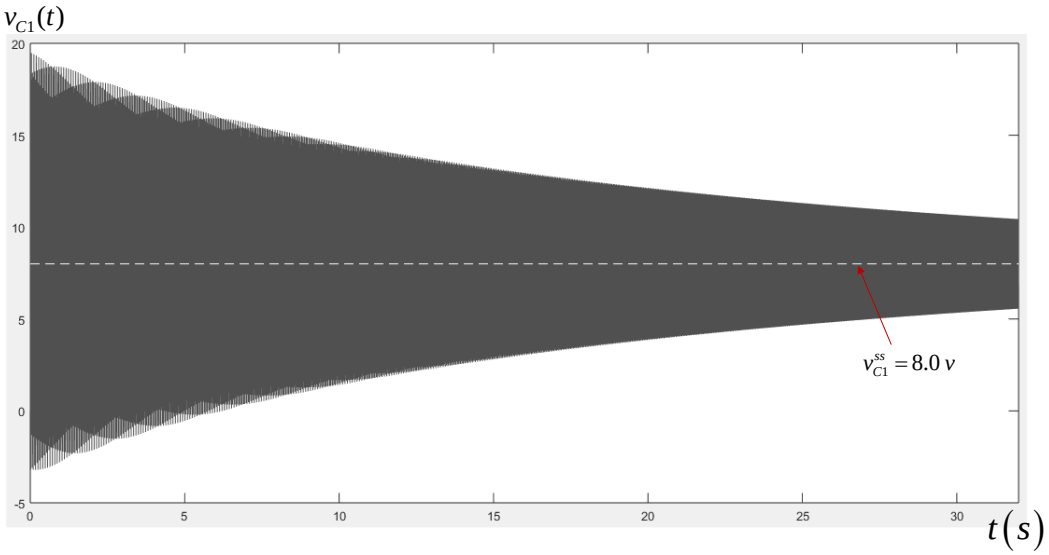

Fig. 7. $v_{C1}(t)$ of a SEPIC in DCM when $v_{out}^{ref} = 5.0\,v$ and $v_s = 8.0\,v$

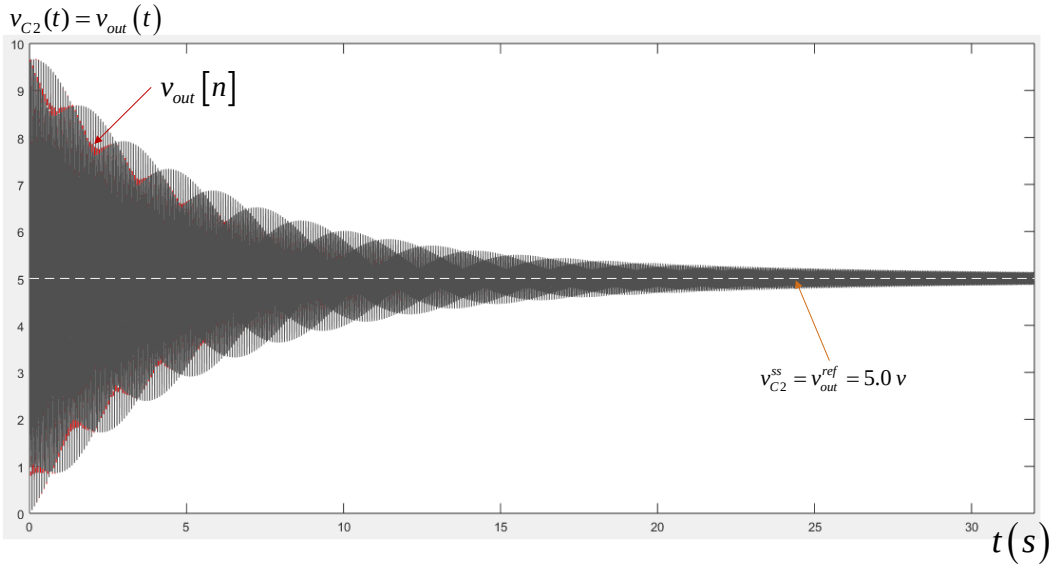

Fig. 8. $v_{C2}(t) = v_{out}(t)$ from the simulation of a SEPIC in DCM and the step response $v_{out}[n]$ from $G_{vu}(z)$ and $G_{v\beta_1}(z)$ for the input sequence $v_s\,u[n]$ and $\beta_1^{ss}\,u[n]$ respectively when $v_{out}^{ref} = 5.0\,v$ and $v_s = 8.0\,v$

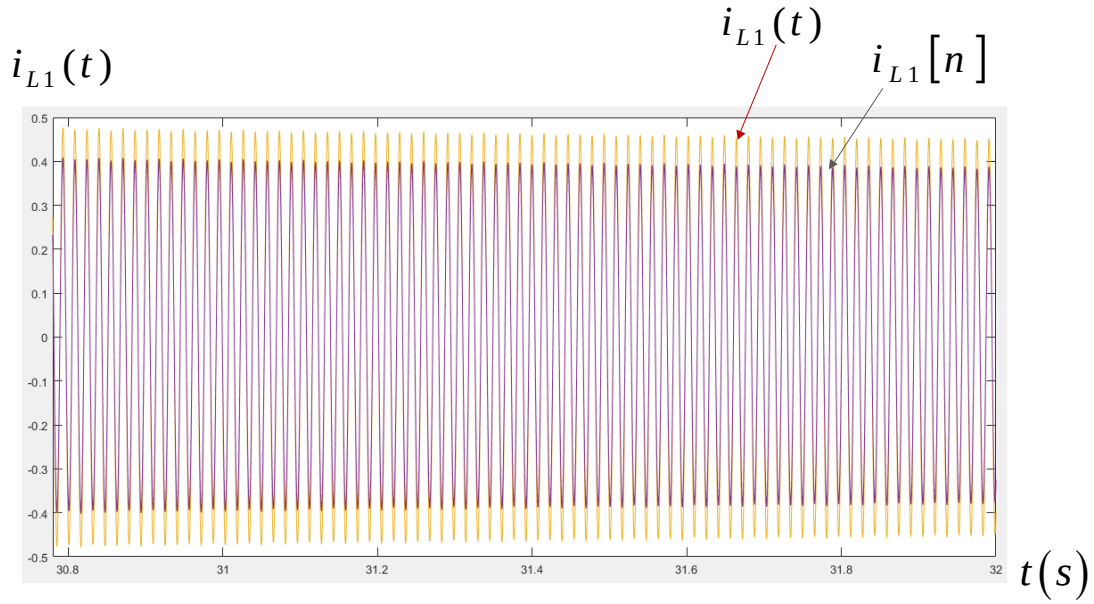

Fig. 9. Enlarged version of $i_{L1}(t)$ (Orange line) from the simulation of a SEPIC in DCM and the step response $i_{L1}[n]$ (violet line) from $G_{vu}(z)$ and $G_{v\beta_1}(z)$ for the input sequence $v_s\,u[n]$ and $\beta_1^{ss}\,u[n]$ respectively when $v_{out}^{ref} = 5.0\,v$ and $v_s = 8.0\,v$ during the steady-state period.

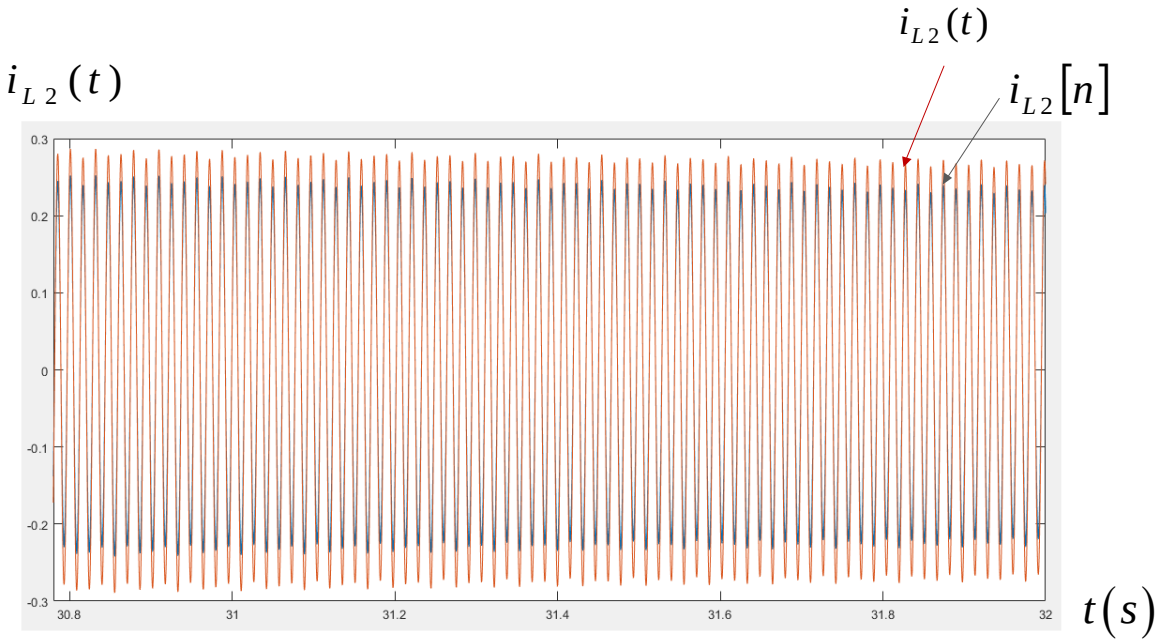

Fig. 10. Enlarged version of $i_{L2}(t)$ (Orange line) from the simulation of a SEPIC in DCM and the step response $i_{L2}[n]$ (violet line) from $G_{vu}(z)$ and $G_{v\beta_1}(z)$ for the input sequence $v_s\,u[n]$ and $\beta_1^{ss}\,u[n]$ respectively when $v_{out}^{ref} = 5.0\,v$ and $v_s = 8.0\,v$ during the steady-state period.

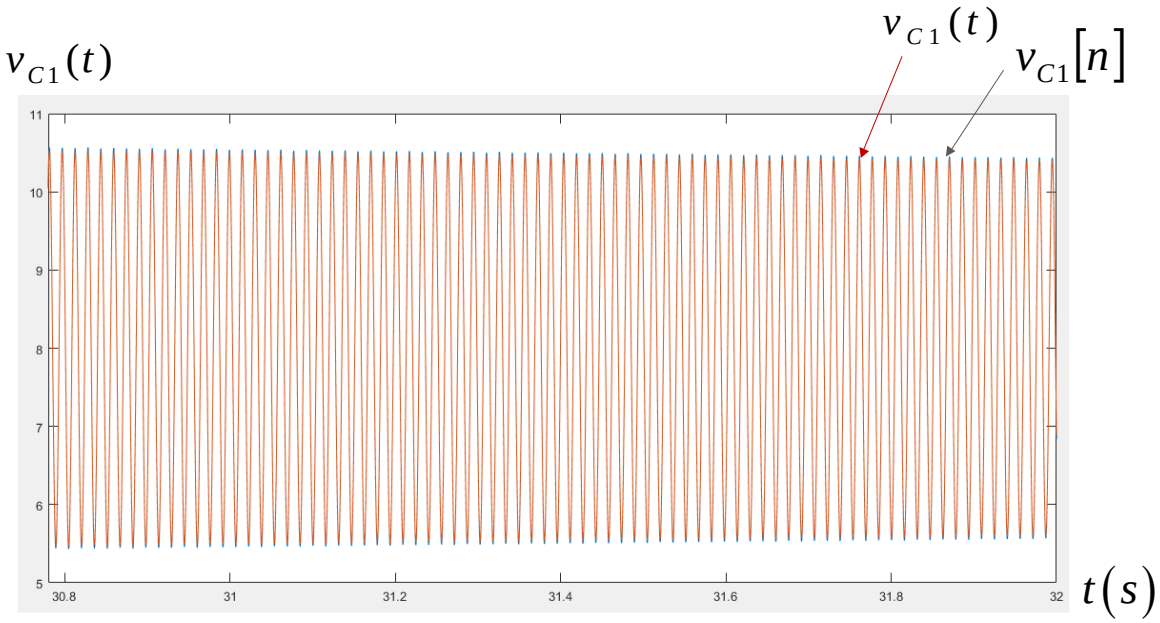

Fig. 11. Enlarged version of $v_{C1}(t)$ (Orange line) from the simulation of a SEPIC in DCM and the step response $v_{C1}[n]$ (violet line) from $G_{vu}(z)$ and $G_{v\beta_1}(z)$ for the input sequence $v_s\,u[n]$ and $\beta_1^{ss}\,u[n]$ respectively when $v_{out}^{ref} = 5.0\,v$ and $v_s = 8.0\,v$ during the steady-state period

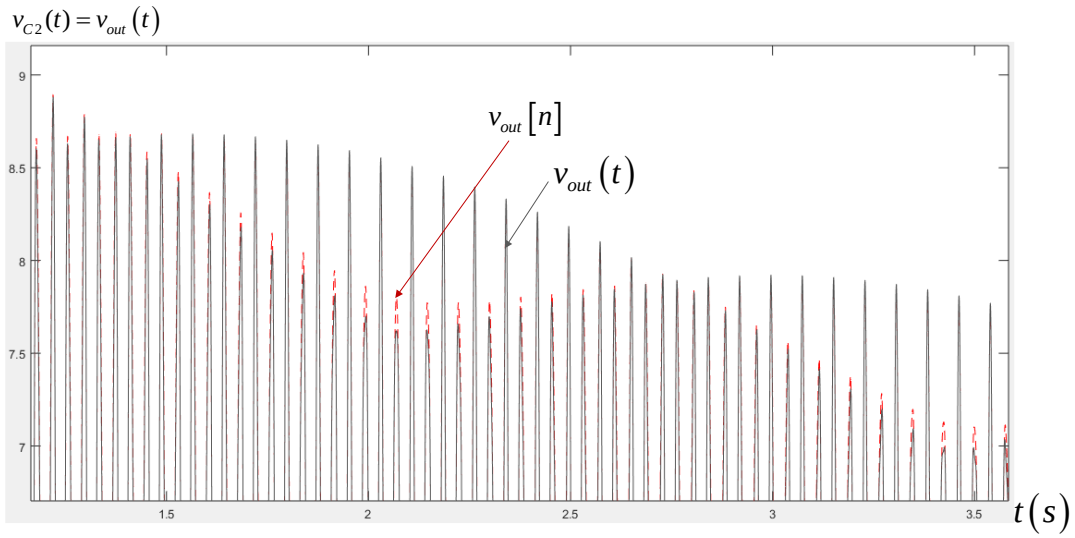

Fig. 12. Enlarged version of $v_{C2}(t) = v_{out}(t)$ (Gray line) from the simulation of a SEPIC in DCM and the step response $v_{out}[n]$ (red line) from $G_{vu}(z)$ and $G_{v\beta_1}(z)$ for the input sequence $v_s\,u[n]$ and $\beta_1^{ss}\,u[n]$ respectively when $v_{out}^{ref} = 5.0\,v$ and $v_s = 8.0\,v$ during the transient period

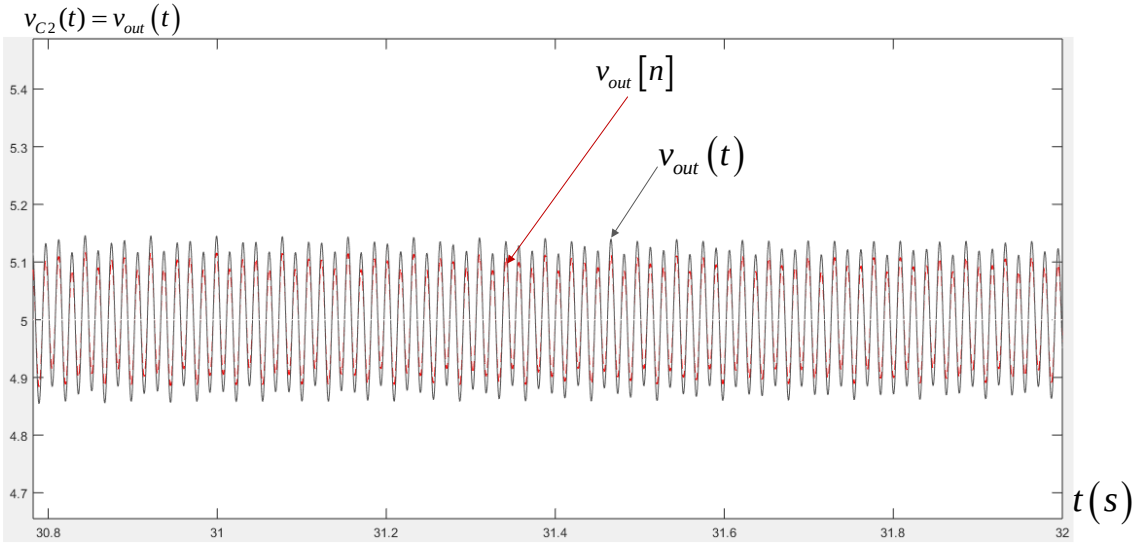

Fig. 13. Enlarged version of $v_{C2}(t) = v_{out}(t)$ (Gray line) from the simulation of a SEPIC in DCM and the step response $v_{out}[n]$ (red line) from $G_{vu}(z)$ and $G_{v\beta_1}(z)$ for the input sequence $v_s\, u[n]$ and $\beta_1^{ss}\, u[n]$ respectively when $v_{out}^{ref} = 5.0\, v$ and $v_s = 8.0\, v$ during the steady-state period

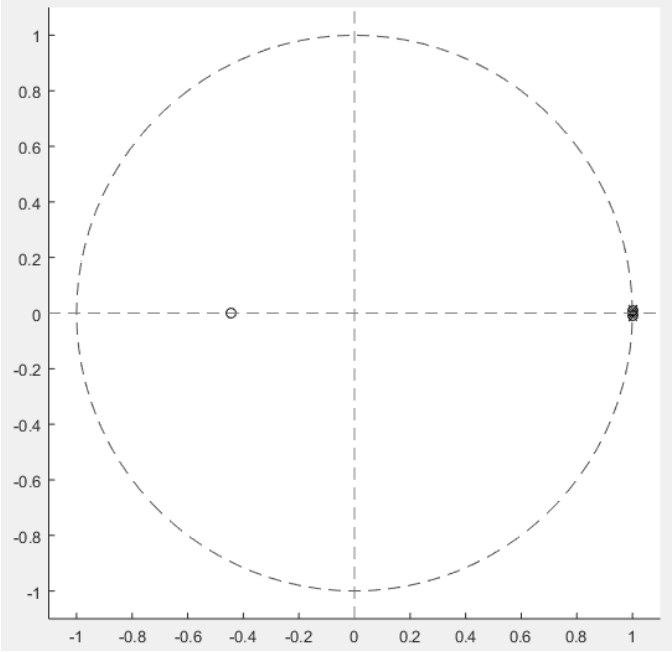

Fig. 14. Pole-zero locations of $T_{vu}(z)$.

Nomenclature

$d(t)$	The switching function.
d_n	The duty ratio.
T_s	The duration of the n^{th} switching cycle.
$\beta_{i,n}(d_{i,n})$	Duty duration in the S_i-state.
A_1	System matrix in the S_1-state .
B_1	Input matrix in the S_1-state.
C_1	Output matrix in the S_1-state.
D_1	Feedforward matrix in the S_1-state.
A_2	System matrix in the S_2-state.
B_2	Input matrix in the S_2-state.
C_2	Output matrix in the S_2-state.
D_2	Feedforward matrix in the S_2-state.
A_3	System matrix in the S_3-state.
B_3	Input matrix in the S_3-state.

C_3	Output matrix in the S_3-state.
D_3	Feedforward matrix in the S_3-state.
L_1, L_2	Inductors in a SEPIC circuit.
C_1, C_2	Capacitors in a SEPIC circuit.
$i_{L1}(t), i_{L2}(t)$	Currents flowing through L_1 and L_2 respectively.
$v_{C1}(t), v_{C2}(t)$	Voltages across C_1 and C_2 respectively.
$v_s, v_{out}, v_{out}^{ref}$	Input, output and desired reference output voltages respectively.
$x_n = x(nT_s)$	State vector at $t = nT_s$.
$x_{n+1} = x((n+1)T_s)$	State vector at $t = (n+1)T_s$.
$x_{ss}\left(u^{ss}, \beta_1^{ss}, T_s\right)$	Steady-state state vector.
u^{ss}	The fixed-point steady-state input vector.
β_1^{ss}	The fixed-point steady-state duty duration in the S_1 state.
$\beta_{1CCM\_MIN}^{ss}$	The minimum value of β_1^{ss} that lastly preserve the SEPIC in CCM.
$v_{out\max\_DCM}^{ss}$	The maximum achievable output voltage for a SEPIC in DCM.
$T_{vu}(z)$	The small-signal input-to-output pulse transfer function.
$T_{v\beta_1}(z)$	The small-signal duty duration-to-output pulse transfer function.
K_{final}	The scaling factor.
$G_{vu}(z)$	The input-to-output pulse transfer function.
$G_{v\beta_1}(z)$	The duty duration-to-output pulse transfer function.

References

[1] Simonetti DSL, Sebastian J, Reis d, Uceda J. Design criteria for SEPIC and Cuk converters as power factor preregulators in discontinuous conduction mode. In Proc. Int. Industrial Electronics, Control, Instrumentation, and Automation Conf.; 1992; San Diego, CA, USA. p. 283-288.

[2] Fang CC, Abed EH. Sampled-Data Modeling and Analysis of PWM DC-DC Converters Part I. Closed-Loop Circuits. Technical research report. MD 20742 USA: INSTITUTE FOR SYSTEM RESEARCH, University of Maryland; 1998. Report No.: T.R. 98-54.

[3] Lee FCY, Iwens RP, Yu. Generalized Computer-Aided Discrete Time-Domain Modeling and Analysis of DC-DC Converters. IEEE Transactions on Industrial Electronics and Control Instrumentation. 1979 May; 26(2).

[4] Kazimierczuk MK. Pulse-width Modulated DC-DC Power Converters: Wiley-Blackwell; 2008.

[5] Middlebrook RD, Cuk S. A GENERAL UNIFIED APPROACH TO MODELLING SWITCHING-CONVERTER POWER STAGES. In Proc. Power Electronics

Specialists Conference, (PESC'76); 1976. p. 19-34.

[6] BROWN R, MIDDLEBROOK RD. SAMPLED-DATA MODELING OF SWITCHING REGULATORS. In Proc. Power Electronics Specialists Conference, (PESC'81); 1981. p. 349-369.

[7] Mayer E, King J. An Improved Sampled-Data Current-Mode-Control Model Which Explains the Effects of Control Delay. IEEE TRANSACTIONS ON POWER 2 ELECTRONICS. 2001; 16.

[8] Cuk S. Modelling, analysis, and design of switching converters. 1976. Dissertation(PhD.), California Institute of Technology.

[9] Simonetti DSL, Sebasti´an J, Uceda J. The Discontinuous Conduction Mode Sepic and ´ Cuk Power Factor Preregulators: Analysis and Design. IEEE TRANSACTIONS ON INDUSTRIAL ELECTRONICS. 1997 OCTOBER; 44(5).

[10] PADHI K. CONTROLLER DESIGN FOR SEPIC CONVERTER USING MODEL ORDER REDUCTION. In ASAR International Conference; 2013; Bangalore, India. p. 51-56.

[11] Cuk , Middlebrook R. A GENERAL UNIFIED APPROACH TO MODELLING SWITCHING DC-TO-DC CONVERTERS IN DISCONTINUOUS CONDUCTION MODE. In IEEE Power Electronics Specialists Conference; 1977; Palo Alto, CA, USA. p. 36-57.

[12] Sun J, Mitchell M, Greuel MF, Krein PT, Bass RM. Averaged modelling of PWM converters operating in discontinuous conduction mode. IEEE Trans. Power Electronic. 1990 May; 16(4).

[13] Chen , Lai JS. Analysis and Design of DCM SEPIC PFC with Adjustable Output Voltage. In Applied Power Electronics Conference and Exposition (APEC); 2015; Charlotte, NC, USA. p. 477-484.

[14] Souvignet T, Allard B, Lin-Shi X. Sampled-Data Modeling of Switched-Capacitor Voltage Regulator With Frequency-Modulation Control. IEEE Transactions on Circuits and Systems I. 2015 April; 62(4).

[15] Vicuna L, Guinjoan F, Majo J, Martinez L. Discontinuous conduction mode in the SEPIC converter. In Proc. Integrating Research, Industry and Education in Energy and Communication Engineering ; 1989. p. 38-42.